RSC Advances

PAPER

View Article Online
View Journal | View Issue

Cite this: *RSC Adv.*, 2017, **7**, 56311

Phase structure and dynamics of polystyrene/poly(vinyl methyl ether) blend studied using solid-state NMR

Yong-jin Peng, *[a] Yu-ling Liu,[a] Jun-hua Hao,[b] Rong-chun Zhang[c] and Ping-chuan Sun[c]

Received 10th November 2017
Accepted 2nd December 2017

DOI: 10.1039/c7ra12287j

rsc.li/rsc-advances

In this work, solid-state ^{1}H NMR experiments were conducted to fully characterize the dynamic characteristics of a polystyrene/poly(vinyl methyl ether) blend with a mass ratio of 3 : 1 (PS/PVME 75/25). About 13% of whole PS was determined to locate in the mobile fraction of the PS/PVME 75/25 blend at room temperature. Increasing the temperature of this blend revealed three transitions. These results are expected to improve our understanding of the glass transition process in polymer systems.

I. Introduction

A polymer blend (polymer alloy) is a multicomponent system of two or more components with different chemical structures and properties. It can display properties differing from those of its individual components due to the interactions between the components.[1–6] Therefore the study of the relationship between the polymer blend structure and properties is very important. There have been many such studies of PS/PVME blends.[7–14]

The PS/PVME blend is a typical lower critical solution temperature (LCST)-type polymer blend, and has garnered much attention, and many studies of its thin film and the properties of this blend doped with materials such as SiO_2, carbon nanotubes and so on have been carried out.[15–20]

Several experiments have shown the weak hydrogen bonds between the oxygens of PVME and aromatic hydrogens of PS to be the source of the compatibility of the PS with PVME in their blend.[10–13] This hydrogen bonds interaction explains the dependence of the compatibility of PS with PVME on the solvent of their blend. Wagler *et al.*[21] used wide-line separation (WISE) experiments to reveal the presence of heterogeneities from 3.5 nm to greater than 30 nm within the PS/PVME blends, depending on the temperature of the heat treatment. The relaxation dynamics of PVME in miscible blends with PS at several concentrations under a broad range of pressure and temperature values were studied by Schwartz *et al.*[13] using dielectric spectroscopy. Recently our group investigated the effect of the interaction between PS and PVME on the glass transition process of the blend at the micro-level using Fourier Transform Infrared Spectroscopy (FTIR).[22]

As a continuation of our previous work,[22,23] we utilized the solid state nuclear magnetic resonance (SSNMR) technique combined with Differential Scanning Calorimetry (DSC) to investigate the phase structure and glass transition process of the PS/PVME blend. Owing to the high resolution of the NMR technique, structural and dynamic information of the blend can be obtained at the micro-level. This article is organized as described below.

First, phase structure information at room temperature was successfully obtained by carrying out dipolar filter ^{1}H spin-diffusion experiments. Then, the evolution of the rigid part of the blend with temperature was elucidated by carrying out variable-temperature ^{1}H double quantum filter (DQF) and Combined Rotation and Multiple Pulse Sequences (CRAMPS) experiments. Our experiments provided a molecular picture for understanding the relationships between the structure and properties and glass transition process of the PS/PVME blend.

II. Experiment

Materials and sample preparation

Polystyrene with a molecular weight of about 110 kg mol^{-1} was purchased from Polymer Source (Canada) and used directly. Poly(vinyl methyl ether) with a molecular weight of 67 kg mol^{-1} in a 50% methanol solution was purchased from TCI Company (Japan) and used after its methanol was removed. PS/PVME with a 3 : 1 mass ratio was dissolved in a toluene solution to a concentration of 1% (g ml^{-1}) and was magnetically stirred at room temperature for 24 hours until it completely dissolved. The solution was rotary evaporated to yield less solvent, and then put in a vacuum oven at a temperature of 40 °C for a week and then at 60 °C for more than two days until its mass no longer changed. A transparent blend film was obtained and differential scanning calorimetry (DSC) results showed good compatibility between the PS and PVME in this blend.

[a]*Teaching and Research Section of Physics, College of Comprehensive Studies, Jinzhou Medical University, Jinzhou 121001, P. R. China. E-mail: hunterpyj2016@163.com*
[b]*Department of Physics, Tianjin University Ren'ai College, Tianjin 301636, P. R. China*
[c]*College of Chemistry, Nankai University, Tianjin 300071, P. R. China*

DSC

The DSC thermograms were obtained using a Mettler-Toledo DSC1 STARe calorimeter. Before taking the measurements, the temperature and heat flow were calibrated. The procedure and results of the DSC experiment for the PS/PVME 75/25 blend and its corresponding pure original species were reported in detail in our previous work.[22]

Solid-state nuclear magnetic resonance

A frequency of 399.72 MHz for the protons was used in our NMR experiments, which were performed on a Varian Infinitplus-400 wide-bore (89 mm) NMR spectrometer with a CP/MAS T3 probe having a rotor diameter of 4 mm. The ^{1}H 12-pulse dipolar filter (DF) and double quantum filter (DQF) experiments under static conditions were performed for the PS/PVME blend over a wide temperature range.

The magic angle spinning (MAS) speed was automatically controlled to be 9.8 kHz ± 1 Hz by using an MAS speed controller for the ^{1}H CRAMPS experiment. The temperature was calibrated with $PbNO_3$ and controlled by using a Varian model-L950 temperature controller. The fractions of rigid and mobile components in the system at a given temperature were derived from the signal intensities of, respectively, ^{1}H DQF and DF spectra at specified filter strengths. For each proton NMR experiment, the number of scans was generally between 24 and 32. The SSNMR pulse sequences are briefly described and shown in Fig. 1.

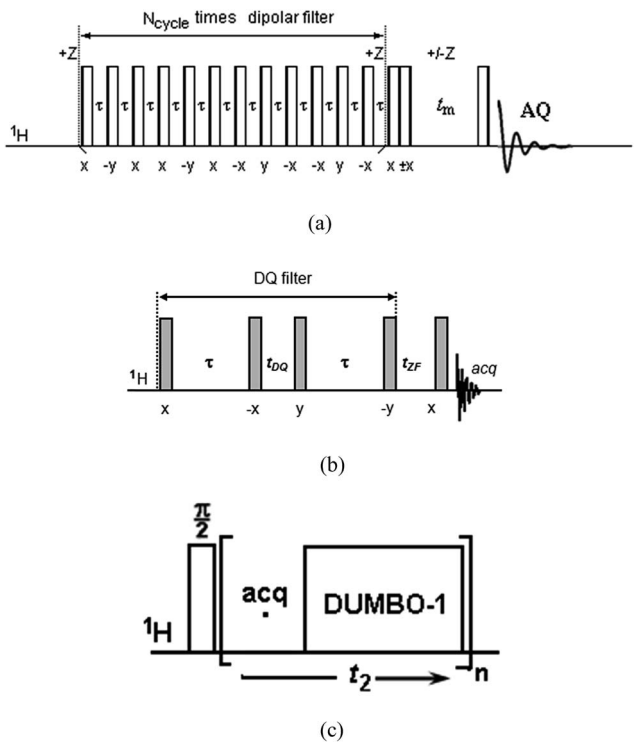

Fig. 1 (a) ^{1}H spin diffusion measurement with only ^{1}H magnetization of the mobile phases selected by a 12-pulse dipolar filter. (b) ^{1}H double-quantum filter (DQF) experiment. (c) ^{1}H combined rotation and multiple pulse spectroscopy (CRAMPS) experiment.

(1) ^{1}H DF experiments.[24,25] The magnetizations of mobile protons with weak dipolar coupling and long relaxation times were selected and used to represent the dynamics of mobile components of PS/PVME blend in this experiment (Fig. 1a). A 12-pulse dipolar filter sequence was used in our work, which guaranteed the selection of the component with high mobility. So the ^{1}H magnetization from the mobile phase, which showed a longer transverse relaxation time than did the rigid phase, was selected from several cycles of a 12-pulse dipolar filter sequence. The selected ^{1}H signals were detected by a 90° ^{1}H pulse as shown in Fig. 1a. The 90° ^{1}H pulse length was 2.5 μs and the inter-pulse spacing τ was 10 μs.

(2) ^{1}H DQF experiments.[26] The magnetizations of rigid protons with strong dipolar coupling were selected and used to determine the dynamics of the glassy component of the PS/PVME blend in this experiment (Fig. 1b). A duration of 10 μs was selected for the DQF excitation and reconversion time (τ) and a duration of 3 μs was selected for the ^{1}H DQF evolution time (τ_{DQ}). With these parameters, the magnetizations of the protons with strong dipolar coupling between each other and related to the rigid components of PS/PVME blend would pass through the filter, whereas that of the weaker dipolar coupling between each other and related to the mobile components would be filtered out.

(3) ^{1}H CRAMPS experiments.[27,28] The ^{1}H CRAMPS method is a technique used to obtain high-resolution solid-state ^{1}H NMR spectra. The DUMBO-1 pulse[29,30] sequence was used for achieving homonuclear decoupling of ^{1}H (Fig. 1c). The 90° pulse width was 2.5 μs. The rotational frequency was automatically controlled to be 9.8 kHz ± 1 Hz. The pulse interval time of DUMBO-1 was set at 0.375 μs. Tetramethylsilane (TMS) was used as an external standard. The ^{1}H chemical shift was calculated with a scaling factor of 0.39 (theoretical value: 0.385) in our experiments, which was determined experimentally. Experimental errors of the ^{1}H chemical shifts were estimated to be less than 0.1 ppm in the range 0–15 ppm.

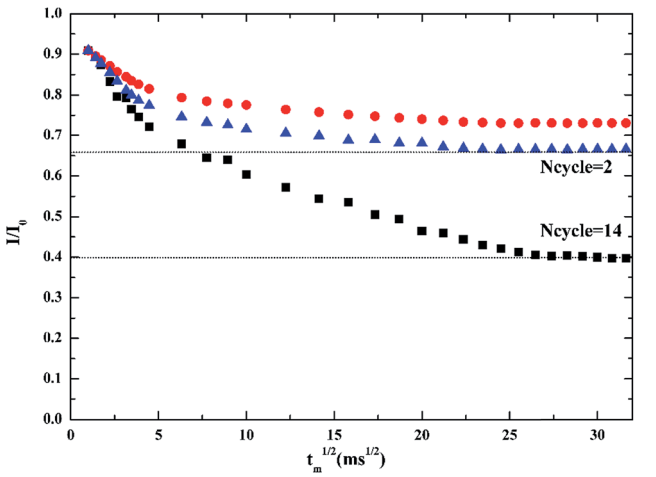

Fig. 2 Static ^{1}H spin-diffusion curve for PS/PVME 75/25 at room temperature.

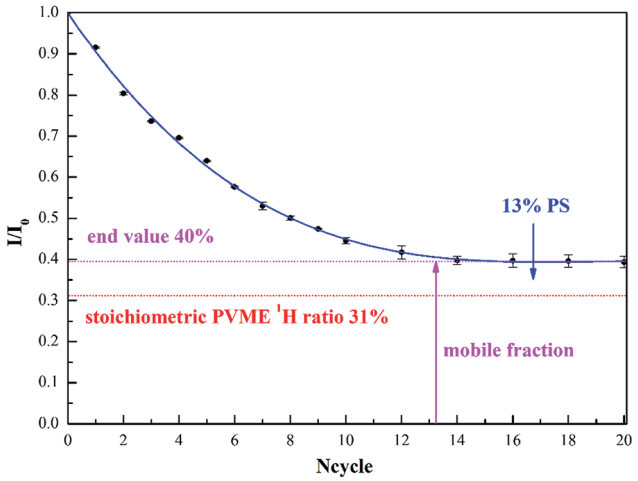

Fig. 3 Selected ^{1}H fraction as a function of filter strength (N_{cycle}) for PS/PVME 75/25 at room temperature. The error bars represent the distributions of the experimental data.

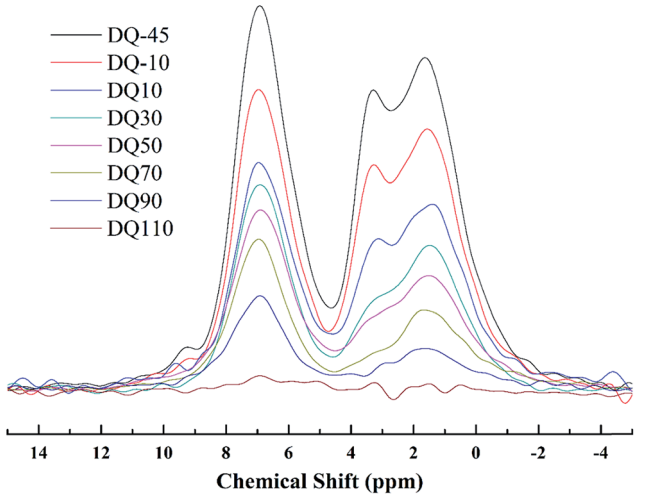

Fig. 5 Double quantum filter ^{1}H CRAMPS of PS/PVME 75/25 at various temperatures, in degrees celsius.

III. Results and discussion

Compatibility of the PS with PVME

The compatiblity of the PS with PVME was large when dissolved in toluene. The glass transition of the PS/PVME blend showed a wider temperature range than did the homopolymer due to the self-concentration effect (see Fig. 1 in ref. 22 and Fig. 6a in this work). This result indicated the presence of a weak interaction between PS and PVME. Our result was consistent with the previous conclusion published by others.[11,12,31,32]

Phase structure of the PS/PVME 75/25 blend

Use of a proton dipolar filter combined with spin diffusion is an effective NMR method, and was used to characterize the microscale phase separation in the polymer system. As shown in Fig. 2, the ^{1}H signal intensity reached an constant value as the diffusion time was increased due to the spin diffusion between the protons at each fixed N_{cycle} value (the bigger the N_{cycle} value, the larger was the dipolar filter strength). The ratio of the final ^{1}H signal intensity to the initial selected ^{1}H signal intensity was found to be equal to the ratio of the initial selected ^{1}H signal intensity to the whole ^{1}H signal intensity in the blend. This ratio decreased as the dipolar filter strength was increased, and reached an constant value finally when N_{cycle} was larger than 14 for PS/PVME 75/25 blend at room temperature as shown in Fig. 3.

The final value of 40%, shown in Fig. 3, indicated the percentage of PS/PVME 75/25 blend at room temperature consisting of mobile components. This proportion exceeded the stoichiometric ^{1}H ratio of the PVME blend by 9%. This result indicated the presence of an interphase in PS/PVME 75/25 and there were some PS components in the interphase at room temperature. This interphase was crucial to the properties of the system. About 13% of whole PS was determined to locate in the mobile fraction of the PS/PVME 75/25 blend at room temperature.

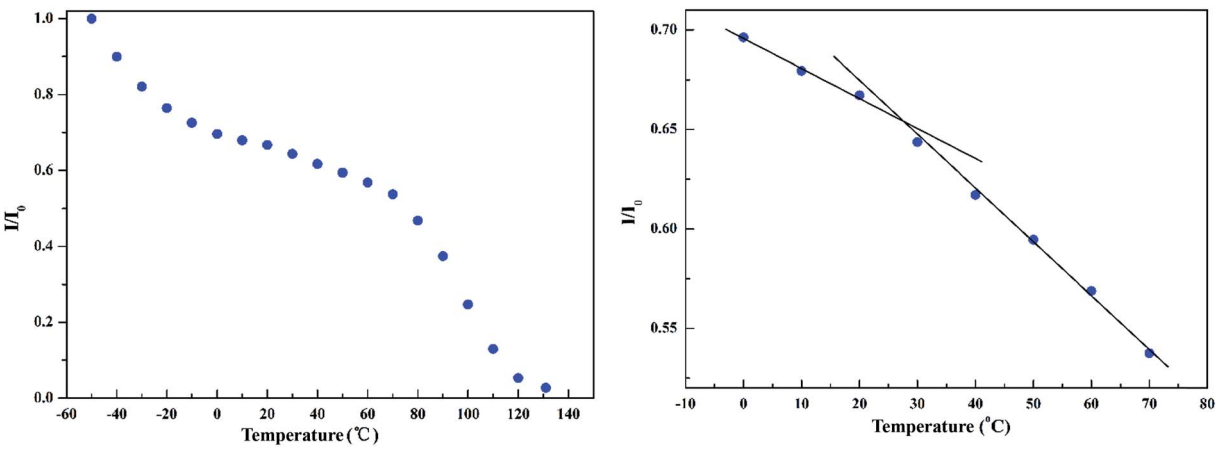

Fig. 4 Normalized intensity of ^{1}H DQF of PS/PVME 75/25 as a function of temperature.

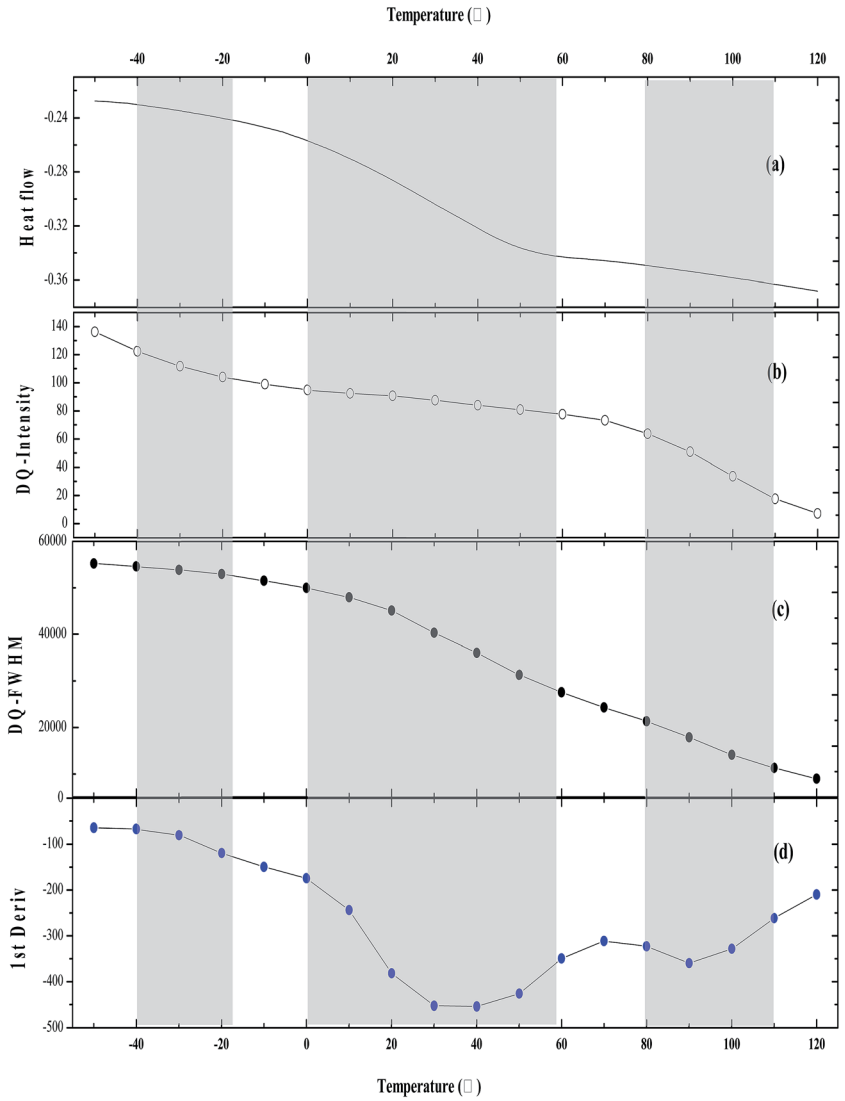

Fig. 6 Comparison of the SSNMR and DSC experimental results for 75/25 PS/PVME. (a) DSC traces (second heating scan). (b) Temperature dependence of the ^{1}H DQF intensities in arbitrary units. (c) Temperature dependence of ^{1}H DQF FWHM. (d) First derivative of the curve in (c). The three shaded regions in the figures indicate three temperature transition regions.

Dynamic characteristics of PS/PVME 75/25

In the calorimetric glass transition temperature range of the blend (about 0–60 °C, see Fig. 6a), the ^{1}H DQF signal intensity of PS/PVME 75/25, which reflected the rigid phase, just showed small variations (as shown in Fig. 4). But near the corresponding PVME glass transition temperature (−25 °C), the ^{1}H DQF signal intensity clearly dropped. This drop was related to the reduction of the dipolar coupling between protons in PVME due to its having become softer as the temperature was increased. However, the whole blend system was still in a glassy state because most of the PS phase was still rigid in this temperature range. So the total ^{1}H DQF signal intensity was still very large.

The specific heat capacity of the blend showed a steep change during the glass transition temperature range of the system whereas the change of the ^{1}H DQF signal intensity was less in this temperature range than in other temperature ranges. This comparison indicated that the glass transition process evaluated using DSC corresponded to a rigid network collapse process (percolation process) rather than a melting process.[23,33,34] In the calorimetric glass transition temperature range, the rigid components of the PS/PVME 75/25 blend were mainly the segments of PS (near 7 ppm corresponding to ^{1}H in the benzene ring) and some PVME segments (near 3.2 ppm corresponding to ^{1}H in the methoxy group) whose mobility was limited by PS as shown in Fig. 5. In this temperature range, most of the connections between the rigid parts of the polymer system were broken but many rigid parts did not yet become soft.

After the percolation process, the system gradually entered into a rubber-like state and the specific heat capacity of the system did not obviously change any longer. Most of the rigid parts of the blend started to become soft when the temperature was increased, which led to the dramatic drop of the ^{1}H DQF

signal intensity. The system finally became a liquid, with a very high mobility.

In order to show the dynamic characteristics of the PS/PVME 75/25 blend more clearly, the DSC curve, the intensity and full width at half maximum (FWHM) of the ^{1}H DQF curve with respect to the temperature are shown in Fig. 6.

Note that in both the temperature ranges −40 °C to −20 °C and 80 °C to 110 °C, the ^{1}H DQF intensity of PS/PVME 75/25 dropped obviously due to the softening of PVME and PS, respectively (Fig. 6b). Because the proportion of PVME in this blend was small (25% in mass ratio), the softening of PVME did not lead to an obvious increase in mobility for the whole blend. So the FWHM of the ^{1}H DQF curve showed a small change from −40 °C to −20 °C. In contrast, from 0 °C to 60 °C (calorimetric blend glass transition) and from 80 °C to 110 °C, the FWHM of the ^{1}H DQF curve showed a significant decrease due to the high mobility of the system obtained through the rigid network collapse (calorimetric glass transition process) and the melting of the PS components, respectively (Fig. 6c), which was also indicated by the two local minimums in the first derivative of the ^{1}H DQ-FWHM curve (Fig. 6d).

The above experimental results indicated that the whole glass transition of PS/PVME 75/25 blend included two processes as in the PS:[23,33,35] one was the percolation process (calorimetric glass transition process), the other was the softening process of the most rigid component (after the calorimetric glass transition process).

IV. Conclusions

In summary, our 12-pulse dipolar filter ^{1}H spin diffusion experiment results indicated the presence of an interphase in the PS/PVME 75/25 blend, and about 13% of whole PS was determined to locate in the mobile fraction of the PS/PVME 75/25 blend at room temperature.

The ^{1}H DQF and CRAMPS experimental results showed the presence of three temperature transition regions for the PS/PVME 75/25 blend: −40 °C to −20 °C (the softening of a portion of PVME), 0 °C to 60 °C (the rigid network collapse process, calorimetric glass transition) and 80 °C to 110 °C (the melting of the rigid PS component).

Our experiment results provided a picture of the dynamics of the PS/PVME 75/25 blend at the micro level and showed similar dynamic characteristics of the glass transition process of the homopolymer and miscible polymer blend. We expect these results to help us understand the glass transition of the polymer system in a deeper way.

Conflicts of interest

There are no conflicts to declare.

Acknowledgements

This work was financially supported by the National Science Fund for Distinguished Young Scholars (No. 20825416), and the National Natural Science Foundation of China (No. 21374051), 973 program (No. 2012CB821503), PCSIRT (No. IRT1257) and CERS-1-61.

References

1 C. C. M. Ma, H. D. Wu and C. T. Lee, *J. Polym. Sci., Part B: Polym. Phys.*, 1998, **36**, 1721–1729.
2 A. Alegria, D. Gomez and J. Colmenero, *Macromolecules*, 2002, **35**, 2030–2035.
3 S.-C. Chen, S.-W. Kuo, U. S. Jeng, C.-J. Su and F.-C. Chang, *Macromolecules*, 2010, **43**, 1083–1092.
4 C. M. Evans, R. W. Sandoval and J. M. Torkelson, *Macromolecules*, 2011, **44**, 6645–6648.
5 C. M. Evans and J. M. Torkelson, *Macromolecules*, 2012, **45**, 8319–8327.
6 Y. He, B. Zhu and Y. Inoue, *Prog. Polym. Sci.*, 2004, **29**, 1021–1051.
7 P. Xavier and S. Bose, *Phys. Chem. Chem. Phys.*, 2014, **16**, 9309–9316.
8 J. K. Yeganeh, F. Goharpey and R. Foudazi, *RSC Adv.*, 2012, **2**, 8116–8127.
9 S. Koizumi, *Soft Matter*, 2011, **7**, 3984–3992.
10 A. A. Bhutto, D. Vesely and B. J. Gabrys, *Polymer*, 2003, **44**, 6627–6631.
11 M. M. Green, J. L. White, P. Mirau and M. H. Scheinfeld, *Macromolecules*, 2006, **39**, 5971–5973.
12 J. A. Pathak, R. H. Colby, G. Floudas and R. Jerome, *Macromolecules*, 1999, **32**, 2553–2561.
13 G. A. Schwartz, J. Colmenero and A. Alegria, *Macromolecules*, 2007, **40**, 3246–3255.
14 H. Yin and A. Schoenhals, *Polymer*, 2013, **54**, 2067–2070.
15 T. Xia, Y. Qin, Y. Huang, T. Huang, J. Xu and Y. Li, *J. Chem. Phys.*, 2016, **145**, 204903.
16 P. Xavier and S. Bose, *Phys. Chem. Chem. Phys.*, 2015, **17**, 14972–14985.
17 P. Xavier and S. Bose, *Abstracts of Papers of the American Chemical Society*, 2014, vol. 248.
18 T. Xia, Y. Huang, X. Jiang, Y. Lv, Q. Yang and G. Li, *Macromolecules*, 2013, **46**, 8323–8333.
19 P. Xavier and S. Bose, *J. Phys. Chem. B*, 2013, **117**, 8633–8646.
20 N. Li, Y.-J. Huang, T. Xia, Q. Yang and G.-X. Li, *Chem. J. Chin. Univ.*, 2013, **34**, 2896–2902.
21 T. Wagler, P. L. Rinaldi, C. D. Han and H. Chun, *Macromolecules*, 2000, **33**, 1778–1789.
22 Y.-j. Peng, Y.-l. Liu, Q. Wu and P.-c. Sun, *Anal. Sci.*, 2017, **33**, 1071–1076.
23 Y.-j. Peng, C.-t. Cai, R.-c. Zhang, T.-h. Chen, P.-c. Sun, B.-h. Li, X.-l. Wang, G. Xue and A.-C. Shi, *Chin. J. Polym. Sci.*, 2016, **34**, 446–456.
24 F. Mellinger, M. Wilhelm and H. W. Spiess, *Macromolecules*, 1999, **32**, 4686–4691.
25 X. Wang, Q. Gu, Q. Sun, D. Zhou, P. Sun and G. Xue, *Macromolecules*, 2007, **40**, 9018–9025.
26 A. Buda, D. E. Demco, B. Blumich, V. M. Litvinov and J. P. Penning, *ChemPhysChem*, 2004, **5**, 876–883.
27 H. Kimura, S. Kishi, A. Shoji, H. Sugisawa and K. Deguchi, *Macromolecules*, 2000, **33**, 9682–9687.

28 R. A. Santos, R. A. Wind and C. E. Bronnimann, *J. Magn. Reson., Ser. B*, 1994, **105**, 183–187.
29 A. L. Webber, B. Elena, J. M. Griffin, J. R. Yates, T. N. Pham, F. Mauri, C. J. Pickard, A. M. Gil, R. Stein, A. Lesage, L. Emsley and S. P. Brown, *Phys. Chem. Chem. Phys.*, 2010, **12**, 6970–6983.
30 E. Salager, R. S. Stein, S. Steuernagel, A. Lesage, B. Elena and L. Emsley, *Chem. Phys. Lett.*, 2009, **469**, 336–341.
31 S. Luo, L. Wei, J. Jiang, Y. Sha, G. Xue, X. Wang and D. Zhou, *J. Polym. Sci., Part B: Polym. Phys.*, 2017, **55**, 1357–1364.
32 C. Pellerin, R. E. Prud'homme and M. Pezolet, *Macromolecules*, 2000, **33**, 7009–7015.
33 R. P. Wool and A. Campanella, *J. Polym. Sci., Part B: Polym. Phys.*, 2009, **47**, 2578–2590.
34 M. I. Ojovan, *J. Non-Cryst. Solids*, 2013, **382**, 79–86.
35 R. P. Wool, in *6th International Conference on Times of Polymers*, ed. A. Damore, L. Grassia and D. Acierno, 2012, vol. 1459, pp. 5–7.